Characteristics of the Electronic Structures of Diabatically and Adiabatically *Z/E*-Isomerizing Olefins in the T_1 State

Maria Brink,[†] Helene Möllerstedt,[†] and Carl-Henrik Ottosson*,[‡]

Department of Organic Chemistry, Chalmers University of Technology, 412 96 Göteborg, Sweden, and Department of Organic Chemistry, Uppsala University, 751 21 Uppsala, Sweden

Received: September 21, 2000; In Final Form: January 23, 2001

Nonlocal gradient-corrected and hybrid density functional theory (DFT) have been used to calculate T_1 potential energy surfaces (PES), spin densities, and geometries of ethylene and aromatic olefins of various sizes: ethylene (**1**), styrene (**2**), stilbene (**3**), 1,1-diphenylethylene (**4**), 1,4-bis-(1-propenyl)benzene (**5**), 1,3-divinylbenzene (**6**), and 2-(1-propenyl)anthracene (**7**). Calculated properties were used to determine differences in electronic structure of olefins that follow adiabatic vs diabatic *Z/E*-isomerization mechanisms. In the planar T_1 structure, the C═C bond in **1** is elongated to a single bond, but in **7** it remains a double bond, archetypal of excitations in the olefinic bond and in the substituent, respectively. Changes in geometries and spin-density distributions of **2**−**7** reveal that substituent aromaticities vary along the T_1 PES. For systems that isomerize diabatically (e.g., **2**), substituent aromaticity is regained in the 90° twisted structure of the C═C bond (^{3}p*). This leads to stabilization and a minimum on the PES at ^{3}p*. If the substituent of the planar T_1 olefin fully can accommodate the triplet biradical and still remain aromatic as in **7**, aromaticity is instead reduced upon twist to ^{3}p*, so that the T_1 PES has a barrier that is suitable for adiabatic isomerizations. The planar structures of olefins with substituents that are partially antiaromatic in T_1 (e.g., phenyl) can be stabilized by radical accepting groups in the proper positions (e.g., **5**). In summary, our calculations indicate that for an aryl-substituted olefin the structure with the highest substituent aromaticity in T_1 corresponds to the minimum on the T_1 PES of *Z/E*-isomerizations.

Introduction

Photochemical *Z/E*-isomerizations of olefins are important processes in nature.[1−4] Similar to all photochemical processes, such rearrangements proceed by either a diabatic or an adiabatic mechanism on the lowest excited singlet (S_1) or triplet (T_1) energy surfaces (Scheme 1),[1,2] or alternatively, they proceed by a combination of these mechanisms in a dual fashion. In an adiabatic process the *E*-isomer (*E**) has the lowest energy on the excited potential energy surface (PES) and the product is formed in the excited state from where decay to the ground state takes place (**I**). On the other hand, in a diabatic process decay occurs from an intermediate with a perpendicularly twisted structure of the C═C bond (p*), so that the product is formed on the ground-state surface (**II**). In the dual mechanism, decay takes place from both the twisted structure and from the planar excited photoproduct. For triplet state *Z/E*-isomerizations, the shape of the T_1 PES and the relative decay rate constants from ^{3}p* and ^{3}*E** to S_0 are important for which mechanism is followed. Because decay from ^{3}p* is more than 10^3 times faster than from ^{3}*E**, it has been estimated that the ^{3}*E** isomer must be at least 7 kcal/mol below ^{3}p* in energy for the isomerization to proceed in a truly adiabatic sense.[2a]

The adiabatic mechanism is preferable because it allows for quantum chain processes and one-way isomerizations from the *Z*- to the *E*-isomer.[2] Adiabatic photorearrangements in the T_1 state can also be catalyzed by addition of a substance with the right properties.[5,6] Therefore, it is now important to find out what electronic factors determine the shape of the T_1 PES, and thus whether a particular T_1 state *Z/E*-isomerization proceeds by the adiabatic or the diabatic mechanism.

Tokumaru and Arai,[2,7] and Mazzucato, Poggi, and co-workers,[8] found that, in arylethylenes, the properties of the aryl groups are important because those with high triplet energies, E_T, lead to diabatic isomerizations and those with lower E_T (e.g., anthrylethylenes[2,7,9]) give adiabatic isomerizations. Because the energy of ^{3}*E** decreases with decreasing E_T of the aryl group, the gain in energy upon twist of the C═C bond is reduced. In 1,2-disubstituted olefins ArCH═CHR, where one substituent is already an aryl group (Ar), the nature of the second substituent is important for the energy of ^{3}p*.[2,7] When the second substituent R is also an aryl group, ^{3}p* is stabilized compared with when R is an alkyl group.

Triplet-state *Z/E*-isomerizations were also studied computationally.[10−16] The T_1 states of three arylethylenes were calculated by Kikuchi, Tokumaru, and co-workers using restricted open-shell Hartree−Fock (ROHF) theory at the MNDO semiempirical, as well as at the ROHF/STO-3G and ROHF/6-31G(d) ab initio levels.[14] The T_1 states of arylethylenes could be written as a combination of two electron configurations describing excitation localization. When the excitation is localized in the isomerizing C═C bond it is an *olefin-excitation*, and when it is localized in the aromatic ring system it is a *ring-excitation*. For olefins undergoing adiabatic isomerization the excitation is mainly of the ring-excitation type, whereas the contrary is true for those undergoing diabatic isomerizations.

In the field of computations, density functional theory (DFT) has been applied to calculate singlet−triplet energy splittings in a range of molecular systems.[15−19] Recently, we compared

[†] Chalmers University of Technology.
[‡] Uppsala University.

10.1021/jp0034022 CCC: $20.00
Published on Web 03/31/2001

SCHEME 1

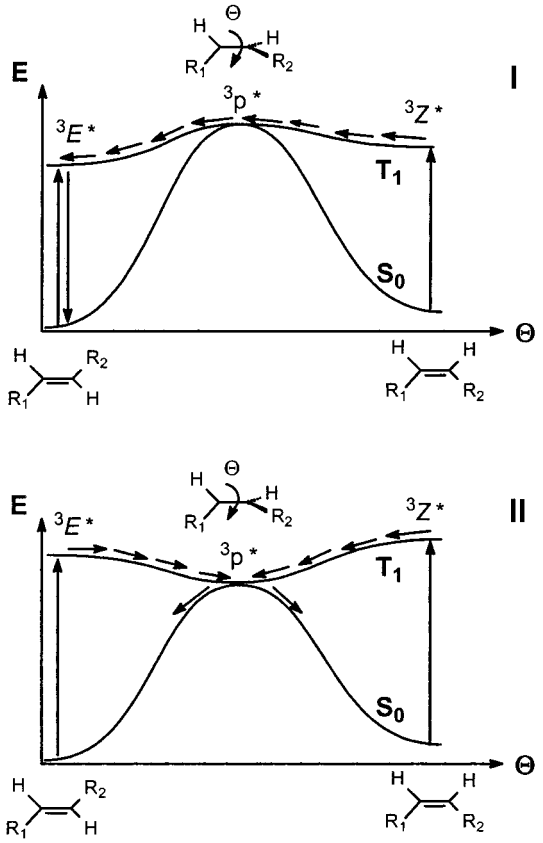

various DFT methods for calculations of T_1 PES of short polyenes.[15] For planar structures, pure nonlocal gradient-corrected methods (e.g., BLYP) gave the best agreement with experimental T_1 energies (within less than 4 kcal/mol), but the overall shape of the T_1 PES calculated by the hybrid density functional methods B3LYP and B3PW91 agree better with the shape of the experimentally estimated surfaces. With regard to geometries, results from hybrid functionals and pure gradient-corrected DFT methods agree better with those from CASSCF, UMP2, and UMP4 than did those from UHF and LSDA calculations.

We now decided to apply one gradient-corrected density functional method (BLYP) and one hybrid density functional method (B3PW91) to a set of olefins, so that information on the electronic structure related to the phenomena of adiabatic and diabatic T_1 state *Z/E*-isomerizations is obtained. How geometries change upon excitation to T_1 will be analyzed, as well as how geometries and spin-density distributions vary along the T_1 PES. Recently, Gogonea et al. published computational results[20] that support the earlier theory of Baird[21] that aromaticity and antiromaticity of *n*-annulenes is reversed when going from S_0 to T_1. For this reason, we specifically analyzed changes in geometries and spin-density distributions along the isomerization pathways in terms of aromaticity changes of the aryl substituents.

The olefins investigated are shown in Scheme 2. This set of molecules makes it possible to investigate various aspects of *Z/E*-isomerizations related to changes in electronic structure. With the set **1-2-3-4** we obtain information on how phenyl groups stabilize planar and perpendicular olefin structures in T_1. Through comparison of **1**, **2**, and **7,** we obtain information on how aryl substituents with low E_T affect geometric and electronic structure of the olefin. This part of the study parallels the previous ROHF investigation of Tokumaru and co-workers,[14] but the calculations are now performed at higher levels of theory. Finally, by comparison of **2**, **5**, and **6** we obtain information on how further substitution at the aryl substituent of an olefin influences the relative stability of planar and twisted olefin structures.

Computational Methods

Both pure nonlocal gradient-corrected and hybrid DFT were used for the investigation of **1**−**7**. For the exchange part either the Becke88 nonlocal gradient-corrected functional (B)[22] or the three-parameter hybrid formula Becke3 (B3)[23] was used, whereas in the correlation part we used either the Lee−Yang−Parr functional (LYP),[24] or the Perdew−Wang (PW91)[25] functional. The basis sets were the 3-21G and 6-31G(d) basis sets of Pople and co-workers, which are of valence double-ζ character.[26,27]

For **1**, the S_0 and T_1 PES were constructed at UBLYP/6-31G(d) and UB3PW91/6-31G(d) levels. However, for **2**−**7**, the T_1 potential energy surfaces were constructed at the UBLYP/6-31G(d)//UBLYP/3-21G and UB3PW91/6-31G(d)//UB3PW91/3-21G levels. Full geometry optimizations with the 6-31G(d) basis set were performed at stationary points corresponding to planar and perpendicular olefin structures. Because we used the spin-unrestricted formalism, computations of S_0 energy curves near perpendicular (biradical) structures give high spin contamination. This will lead to errors in the S_0 energies, and therefore we refrained from computation of S_0 PES of **2**−**7**. Instead, their S_0 PES were only drawn schematically by scaling the S_0 PES of **1**. This neglects the relative order of S_0 and T_1 energies at perpendicular structures; however, because we are primarily interested in the shapes of the T_1 PES, this is not a serious drawback.

Because the spin contamination in the T_1 states is low along the complete twisting motion ($\langle\hat{S}^2\rangle < 2.07$), an analysis of the Mulliken spin-density distribution should be allowed and gives useful results. We used the UBLYP/6-31G(d) density because this method gives the lowest spin contamination.

All computations were performed with the Gaussian94[28a] and Gaussian98[28b] quantum chemical program packages.

Results and Discussion

Calculated triplet energies of the planar conformations of **1**−**7** together with experimental values are collected in Table 1, whereas Table 2 contains energies of perpendicular structures ($^3p^*$) relative to the ground-state *E*-isomers. Geometry data for various conformers of **1**−**7** in both T_1 and S_0 states at (U)B3PW91/6-31G(d) level are summarized in the figures. The Mulliken spin-density distributions at the UBLYP/6-31G(d) level are also found in these figures. Moreover, T_1 potential energy curves for twisting around the isomerizing C=C bonds are plotted. Finally, plots of the Kohn−Sham SOMOs for the T_1 states of the *E*-isomers, based on UBLYP/6-31G(d) calculations, are shown. For numbering of atoms, see figures with optimized geometries.

For stationary points the agreement between single-point UBLYP/6-31G(d)//UBLYP/3-21G and UB3PW91/6-31G(d)//UB3PW91/3-21G energies and those obtained from UBLYP/6-31G(d) and UB3PW91/6-31G(d) optimizations is within 0.3 kcal/mol (Tables 1 and 2). It is thus justified to base the T_1 PESs on single-point energies. The 6-31G(d) basis set was sufficient in DFT calculation of S_0-T_1 energy splittings in shorter polyenes, and neither correlation-consistent or larger basis sets alter the results significantly.[15]

SCHEME 2

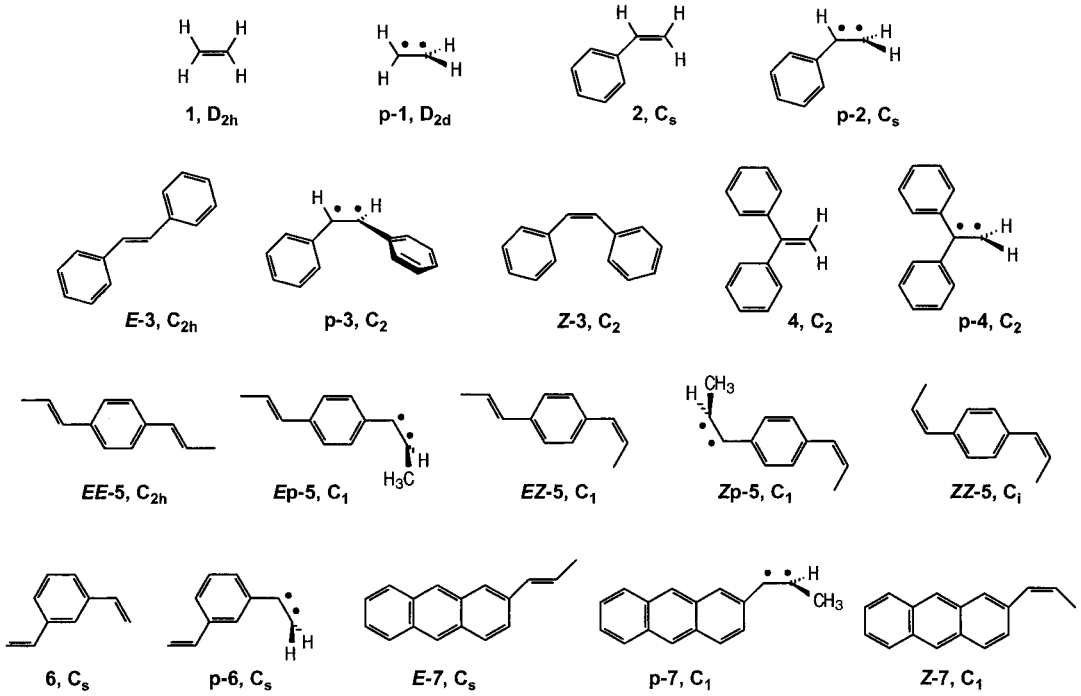

TABLE 1: T_1 Energies of Planar Isomers of 1−7 Relative to the Respective S_0 *E*- and *Z*-Isomers[a]

substance	symmetry	experiment	UBLYP/6-31G(d)// UBLYP/3-21G	UBLYP/6-31G(d)[b]	UB3PW91/6-31G(d)// UB3PW91/3-21G	UB3PW91/6-31G(d)	ROHF/6-31G(d)
1	D_{2h}	84.0[c]	84.9	84.9	80.7	80.6	62.1
2	C_s	60.8−64.9[d,e]	61.2	61.2	61.3	61.3	59.4
E-**3**	C_{2h}	51.0[d]	47.8	47.7	48.8	48.7	52.1
Z-**3**	C_2	55.5[d]	50.1	50.0 (55.6)	51.8	51.8 (56.5)	51.3 (54.8)
4	C_2	60.8[d]	58.1	58.1	58.9	58.9	55.9
EE-**5**	C_s	55.4[f]	50.2	50.1	52.3	52.3	55.6
EZ-**5**	C_1	56.2[f]	50.7	50.8 (53.8)	53.4	53.4 (56.0)	55.8
ZZ-**5**	C_1	56.4[f]	51.1	51.4 (57.4)	54.0	54.2 (59.6)	56.1
6	C_s	−	61.2	61.2	61.9	61.8	56.9
E-**7**	C_s	41.6−42.5[g]	39.1	39.2	41.7	41.5	40.0
Z-**7**	C_1	41.6−42.5[g]	38.2	38.3 (42.0)	40.1	40.2 (43.4)	38.8 (42.1)

[a] Energies in kcal /mol. [b] Energies of T_1 excited *Z*-isomers relative to ground state *E*-isomers are given in parentheses. [c] Value from ref 29. [d] Value from ref 31. [e] Value from ref 32. [f] Value from ref 41. [g] Values from ref 9 taken as the interval spanned by 2-ethenylanthracene and 2-(3,3-dimethyl-1-butenyl)anthracene.

TABLE 2: T_1 Energies of ^{3}p* Structures of 1−7 Relative to the S_0 *E*- or *EE*-Isomer[a]

substance	symmetry	experiment	UBLYP/6-31G(d)// UBLYP/3-21G	UBLYP/6-31G(d)	UB3PW91/6-31G(d)// UB3PW91/3-21G	UB3PW91/6-31G(d)	ROHF/6-31G(d)
p-**1**	D_{2d}	(62.6)[b]	65.6	65.6	62.0	61.9	46.7
p-**2**	C_s	51.2[c]	55.8	55.7	53.0	52.9	42.9
p-**3**	C_2	46.5[c]	46.8	46.7	44.7	44.6	39.4
p-**4**	C_2	52.1[c]	52.8	52.9	50.8	50.9	43.4
E,p-**5**	C_1	56.8[d]	53.8	53.7	51.6	51.5	43.1
Z,p-**5**	C_1	58.9[d]	57.2	57.0	54.9	54.6	46.0
p-**6**	C_s	−	56.1	56.1	53.2	53.2	42.9
p-**7**	C_1	52.6−53.5[e]	53.8	53.6	51.4	51.2	43.7

[a] Energies in kcal/mol. [b] Value refers to MRD-CI from ref 30. [c] Value from ref 31. [d] Value from ref 41. [e] Value from ref 9.

Ethylene (1). The T_1 energy calculated for **1** at UBLYP/6-31G(d) and UB3PW91/6-31G(d) levels agrees well with the experimental value (Table 1).[29] However, the triplet energy for the perpendicular structure at UBLYP/6-31G(d) level (65.6 kcal/mol) is slightly higher than the value obtained by Gemein and Peyerimhoff (62.6 kcal/mol)[30] when using multireference determinant configuration interaction (MRD-CI). The energy calculated at UB3PW91/6-31G(d) level is in better accordance with that of MRD-CI. The result from the ROHF calculation disagrees with those from DFT and MRD-CI.

The energy gain for rotation of the C═C bond is 19.3 kcal/mol at UBLYP/6-31G(d) level, 18.7 kcal/mol at UB3PW91/6-31G(d) level, and 16.2 kcal/mol at MRD-CI level.[30] Disregarding these small energy differences, the T_1 energy surface of **1** (Figure 1) is archetypal of olefins following a diabatic isomerization mechanism, and the energy drop is taken as a reference for what is possible for an isomerization where the T_1 state is completely composed of an olefin excitation.

The length of the double bond increases by 0.208 Å upon triplet excitation of planar **1** (Figure 2), so that it adopts the

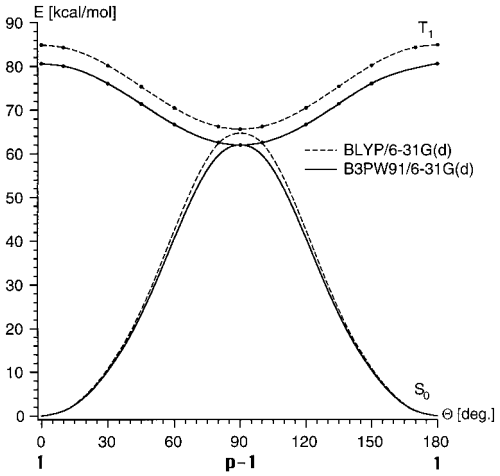

Figure 1. S_0 and T_1 potential energy surfaces for rotation around the C═C bond in **1** computed with UBLYP/6-31G(d) (dashed lines) and UB3PW91/6-31G(d) (solid lines).

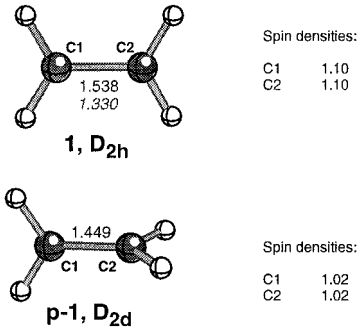

Figure 2. Geometries of ethylene (**1**) calculated at (U)B3PW91/6-31G(d) level, with values for the T_1 state in normal print, and values for the S_0 state in italics. Mulliken spin densities computed at UBLYP/6-31G(d) level. Positive values of the atomic spin density refer to α-spin expressed in electrons.

length of a single bond. The excitation in ethylene represents an ideal olefin excitation, because the second SOMO in **1** is the pure π^* orbital localized to the isomerizing C═C bond. Because the T_1 state is mainly composed of the configuration with one electron lifted from the highest occupied molecular orbital (HOMO) to the lowest unoccupied molecular orbital (LUMO), the bond elongation in **1** is the maximum elongation that can occur for an olefin when excited to T_1. Upon twist the C═C bond is shortened by ∼0.1 Å, presumably a result of stabilizing hyperconjugative interactions between the singly occupied 2pπ(C) atomic orbitals (AO) and the empty pseudo-$\pi^*(CH_2)$ orbitals.

Styrene (2). Stabilization of the planar T_1 structure of an olefin is achieved through delocalization of the two unpaired α-electrons away from the isomerizing C═C bond. In this regard, we study the influence of a phenyl substituent, leading to **2**. To what extent does such substitution alter the electronic structure of the olefin, and what connection is there between electronic structure and shape of the T_1 PES? To answer these questions we analyze changes in geometries and spin-density distributions because these indicate how certain points on the T_1 PES of **2** are stabilized when compared with **1**.

The T_1 energies for planar styrene calculated with UBLYP/6-31G(d) and UB3PW91/6-31G(d) are in the lower part of the experimental range (Table 1). However, the calculated triplet energies for p-**2** are higher than found in measurements (energy lowering upon twist at UBLYP/6-31G(d), 5.5 kcal/mol; at UB3PW91/6-31G(d), 8.4 kcal/mol; and experimentally,[31,32] 9.6−13.7 kcal/mol). Thus, as noted previously for 1,3-butadiene and 1,3,5-hexatriene,[15] UBLYP underestimates the stability of ^{3}p* structures. Correction for zero-point vibrational energy does not change the energy difference between the planar and perpendicular structures of **2** because it is 8.3 kcal/mol at UB3PW91/6-31G(d) level. The calculated difference in ΔH(298 K) is 9.0 kcal/mol at the same level of theory. Because DFT results agree well for the other olefins (vide infra), we are convinced that especially UB3PW91 also gives correct energies for **2**.

Several computational studies on the singlet-state photochemistry of styrene have been reported.[33] With regard to the T_1 photochemistry, semiempirical calculations were performed by Said and Malrieu[10] and by Tokumaru, Kikuchi, and coworkers.[14a] The latter also performed ROHF calculations with the STO-3G and 6-31G(d) basis sets[14b] using ROHF/STO-3G geometries. However, the ROHF/6-31G(d)//ROHF/STO-3G energies are too high by ∼10 kcal/mol when compared with experimental values,[14b] even though the energy gain for C═C twist (14.2 kcal/mol) agrees with the measured value (9.6−13.7 kcal/mol).[31,32] Doubt exists about the correctness of ROHF because use of a better basis set for both geometries and energies gives a larger discrepancy to the experiments (Tables 1 and 2). The performance of ROHF for the other olefins is also not satisfactory. Moreover, because UB3PW91 seems to be slightly better than UBLYP for energies, and because we are mainly interested in the photochemical aspects, we base the discussion of energies and geometries on UB3PW91 data but spin densities on UBLYP data because the UBLYP data give lower spin contamination.

Tokumaru and Arai argued that aryl substituents on the C═C bond lower the triplet energy for the planar olefin, so that when the triplet energy of the Ar group is sufficiently low, the *Z/E*-isomerization proceeds according to the adiabatic mechanism.[2,7] Because the energy difference between planar **1** and **2** in the T_1 state is ∼20 kcal/mol, whereas it is ∼10 kcal/mol between perpendicular **1** and **2**, it is clear that a phenyl group better stabilizes planar than perpendicular olefin structures. As a result, the T_1 PES of **2** (Figure 4) is shallower than that of **1**, even though the planar T_1 structure of **2** is not sufficiently stabilized to correspond to a minimum.

However, because *n*-annulenes that are aromatic in S_0 are antiaromatic in T_1, and vice versa,[20,21] the phenyl group should give **2** some antiaromatic character in T_1, and the stabilization of a planar olefin by a phenyl group should indeed be limited when compared with olefins substituted by other groups. This is supported by a comparison of **2** (phenyl-substituted ethylene) and 1,3-butadiene (vinyl-substituted ethylene), because the latter molecule has a slightly lower experimental triplet energy than **2** (experimental, 59.7 kcal/mol for butadiene[34]; 60.8−64.9 kcal/mol for **2**[31,32]). The difference is more pronounced in the computations; for example, at the UB3PW91/6-31G(d) level the corresponding T_1 energies are 57.1 [15] and 61.3 kcal/mol.

Upon excitation of **2** to T_1 the C1C2 bond is elongated by 0.13 Å at the UBLYP/6-31G(d) level (Figure 5), slightly more than half of the elongation in **1**. The smaller bond elongation in **2** than in **1** correlates with the smaller energy gain upon rotation, and stems from delocalization of the biradical character in planar **2** away from the C═C bond. An analysis of geometry changes within the phenyl group upon excitation to T_1 is rewarding. When compared with the S_0 geometry the C2C3, C4C5, and C7C8 bonds are shortened, whereas the C3C4, C3C8, C5C6, and C6C7 bonds are elongated. Thus, the electronic structure of the T_1 state of planar **2** is mainly described by a quinoid-type resonance structure with the unpaired α-electrons

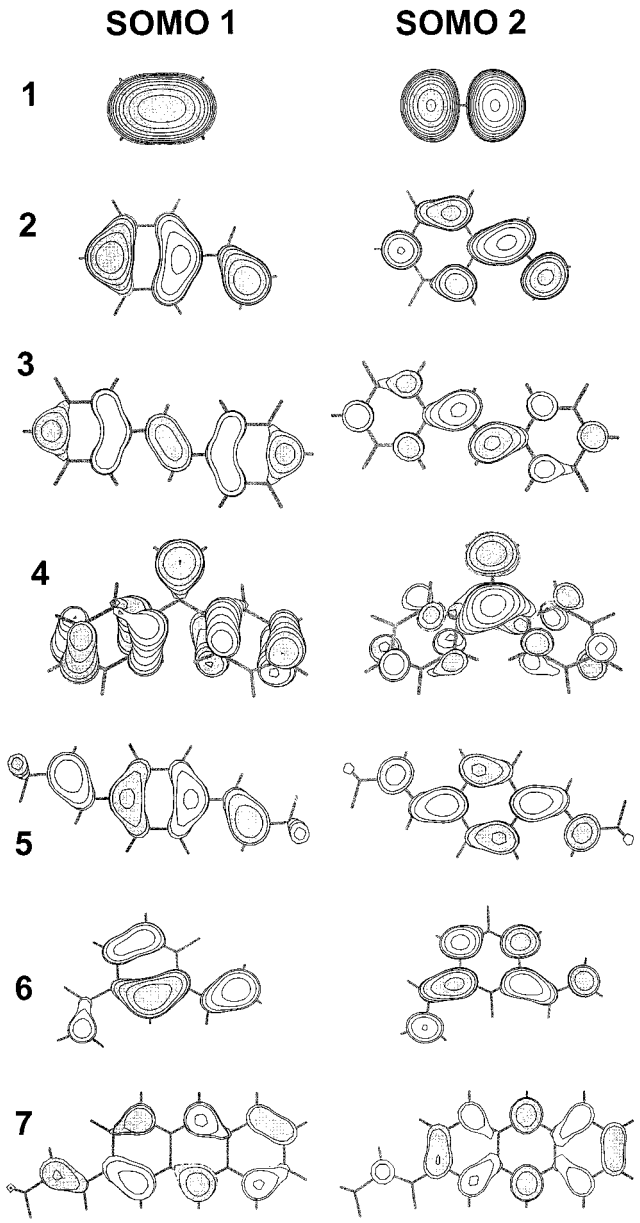

Figure 3. Plots of the two Kohn−Sham SOMOs of **1**−**7** in the T_1 state based on UBLYP/6-31G(d) calculations.

at C1 and C6 (**Ic**; Scheme 3). This finding is supported by the spin-density distribution, because C6 and C1 have the highest α-spin densities (Figure 5), even though some density is also located at C2 and the two ortho-positions C4 and C8.

Upon twist, the CC bonds within the phenyl group equalize, because the difference between the longest and shortest CC bond at the UBLYP/6-31G(d) level decreases from 0.086 to 0.037 Å. These variations should be compared with that in the S_0 geometry (0.015 Å). Thus, during the isomerization process the phenyl group in **2** regains aromaticity, which stabilizes p-**2** over planar **2** and leads to a diabatic isomerization. The resonance structure **IIa**, which is described as a 1,2-biradical with an aromatic phenyl group, should be more important in p-**2** than in planar **2**, and this is supported by the calculated spin density. The spin density at C1 in p-**2** is identical with that in p-**1**. That p-**2** is partially described as a 1,2-biradical agrees with a similar finding by Caldwell and Zhou obtained when investigating the rate for ring opening of cyclopropylcarbinyl-substituted styrenes in the T_1 state.[35] However, p-**2** is also more than just a 1,2-biradical.

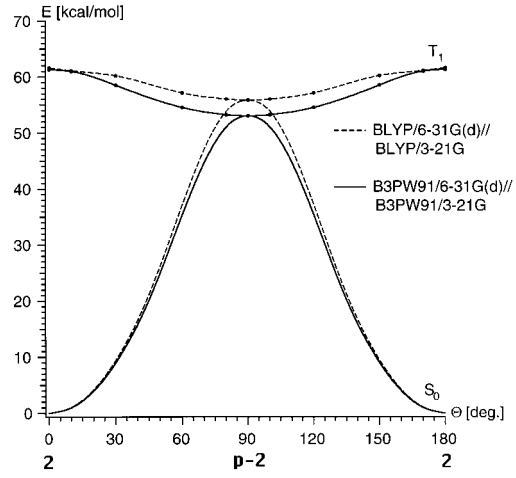

Figure 4. S_0 and T_1 potential energy surfaces for rotation around the C═C bond in styrene (**2**) computed with UBLYP/6-31G(d)//UBLYP/3-21G (dashed lines) and UB3PW91/6-31G(d)//UB3PW91/3-21G (solid lines). The S_0 PES are schematic, interpolated from values of planar and perpendicular geometries.

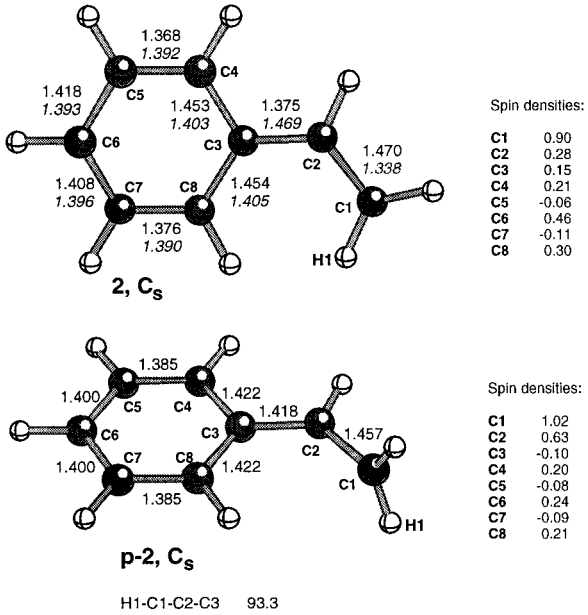

Figure 5. Geometries of styrene (**2**) calculated at the (U)B3PW91/6-31G(d) level, with values for the T_1 state in normal print, and values for the S_0 state in italics. Mulliken spin densities computed at the UBLYP/6-31G(d) level. Positive values of the atomic spin density refer to α-spin expressed in electrons.

Because the excitation to T_1 is a HOMO−LUMO excitation, the shape of the second SOMO of the T_1 state is a rough indicator of excitation localization. Plots of the frontier orbitals in **2** show that this orbital is slightly localized to the isomerizing C═C bond (Figure 3).

Because a phenyl group helps to stabilize primarily planar structures through delocalization of one of the two unpaired electrons away from the olefinic C═C bond, a further delocalization and stabilization should be obtained by additional phenyl substitution as in stilbene (**3**) and 1,1-diphenylethylene (**4**).

Stilbene (3). The triplet energy of *E*-**3** at UB3PW91/6-31G(d) level is lower than found experimentally by 2.3 kcal/mol (Table 1),[31] and the corresponding energy for the *Z*-isomer differs from the experimental estimate on the lower side by 3.7 kcal/mol. Because the calculated energy for p-**3** is 1.9 kcal/mol below the measured energy, the T_1 PES is slightly underestimated by 2−4 kcal/mol. However, the shape of the T_1 PES at UB3PW91

SCHEME 3

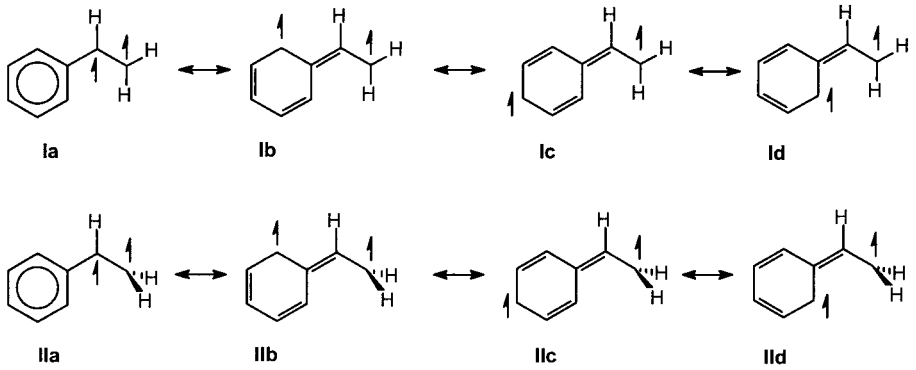

level is in line with the observation that the *Z/E*-isomerization of **3** is diabatic, but that it proceeds on a rather flat T_1 surface between *E*-**3** and p-**3**.[1,31,36−38]

The energy difference between the *E*- and *Z*-isomers in S_0 is 4.8 kcal/mol with B3PW91, whereas in T_1 this difference increases to 7.8 kcal/mol. Thus, steric congestion between the phenyl groups is transferred and even increased in T_1 so that *Z*-**3** becomes a transition state. Because of steric strain the energy drop when going from *Z*-**3** to p-**3** is larger than for *E*-**3**, and it is not representative for changes in the electronic structure. When going from *E*-**3** to p-**3** the energy gain is 4.1 kcal/mol at the UB3PW91/6-31G(d) level, in agreement with the experiment (1.6−4.5 kcal/mol).[31,36] Laser flash photolytic studies by Görner and Schulte-Frohlinde revealed an equilibrium between triplet *E*-**3** and p-**3**,[37] which implies a flat T_1 PES. Resonance Raman spectroscopy further showed a population of *E*-**3** in T_1.[38] According to our calculations, both *E*-**3** and p-**3** are minima with UBLYP/3-21G, but the former is a very shallow transition state at the UB3PW91/3-21G level (ν_1 = 8.4i cm^{-1} when at C_{2h} symmetry).

With phenyl groups in both 1- and 2-positions of the olefin, stabilization of the planar T_1 structure is larger than with one phenyl group. The planar T_1 structure is also stabilized more than ^{3}p* because, according to the DFT calculations, the lowering when going from **2** to *E*-**3** is ∼13 kcal/mol and ∼9 kcal/mol when going from p-**2** to p-**3**. However, 1,2-diphenyl substitution of an olefin is not as efficient in lowering the triplet energy as 1,2-divinyl substitution, because 1,3,5-hexatriene has a lower measured triplet energy than *E*-stilbene (46.9 vs 51.0 kcal/mol).[39,31]

The elongations of the olefinic C═C bond in planar T_1 structures of **3** are similar or slightly smaller than in **2** (0.116 and 0.129 Å in **3** vs. 0.132 Å in **2**; Figures 5 and 7). A more shallow T_1 PES when going from *E*-**3** to p-**3** thus correlates with a less elongated C═C bond. The olefinic bond in T_1 is longer in *Z*-**3** than in *E*-**3** because of steric hindrance, supported by a larger energy difference between *E*-**3** and *Z*-**3** in T_1 than in S_0. Increased steric strain for *Z*-**3** in T_1 is accounted for by quinoid-type resonance structures in which the C2C3 and C1C9 bonds become double bonds, and relief of steric congestion through rotation around these bonds is less facile than in S_0.

A pattern of bond-length changes within the phenyl groups occurs in T_1 that resembles those in **2**, even though the variation in CC bond lengths in *E*-**3** is smaller than in **2** (0.060 vs 0.086 Å, Figures 7 and 5, respectively). The importance of quinoid-type resonance structures also in **3** is supported by the fact that the spin density is highest at C2, C4, C6, and C8 (C1, C10, C12, and C14) in both *E*-**3** and *Z*-**3**, but compared with planar **2** more density is located at C1 and C2.

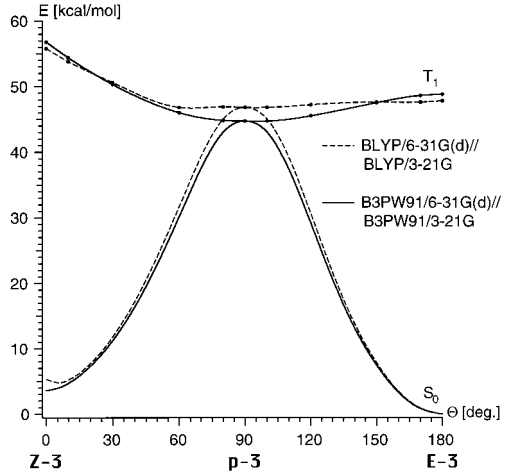

Figure 6. S_0 and T_1 potential energy surfaces for rotation around the C═C bond in stilbene (**3**) computed with UBLYP/6-31G(d)//UBLYP/3-21G (dashed lines) and UB3PW91/6-31G(d)//UB3PW91/3-21G (solid lines). The S_0 PES are schematic, interpolated from values of planar and perpendicular geometries.

When the olefinic bond is rotated, the bond-length variation within the phenyl group decreases to 0.038 Å, indicating that aromaticity is partially regained. However, the bond-length variation is still twice that in the S_0 geometry of *E*-**3** (0.018 Å). The C2C3 and C1C9 bonds also become longer, in line with the reduced importance of the quinoid-type resonance structures. The α-spin density is redistributed to the C1 and C2 atoms, and the density at these atoms resembles that of C2 in p-**2**.

Changes in the electronic and geometric structure that occur upon excitation to T_1 reveal why stilbene isomerizes diabatically, although on a shallower surface than styrene. Due to the diabatic character of the *Z/E*-isomerization of **3**, its T_1 state is still of the olefin-excitation type, confirmed by the shape of the second SOMO (∼LUMO of S_0). This orbital has slightly larger contributions from the 2pπ(C) AOs of the rotating C═C bond than from the phenyl groups (Figure 3).

Through further delocalization of the triplet biradical character away from the C═C bond, even better stabilization of the planar T_1 olefin should be achieved. One could believe initially that attachment of two phenyl substituents at the same C atom would increase such delocalization, and for this reason, we calculated 1,1-diphenylethylene (**4**). Because only one of the two unpaired electrons in this olefin can be delocalized away from the C═C bond, it should be compared with **2**.

1,1-Diphenylethylene (4). The UB3PW91/6-31G(d) energy of the planar T_1 structure is 58.9 kcal/mol, in agreement with the measured value of 60.8 kcal/mol from photoacoustic calorimetry.[31] The measured energy of p-**4** (52.1 kcal/mol)[31] is

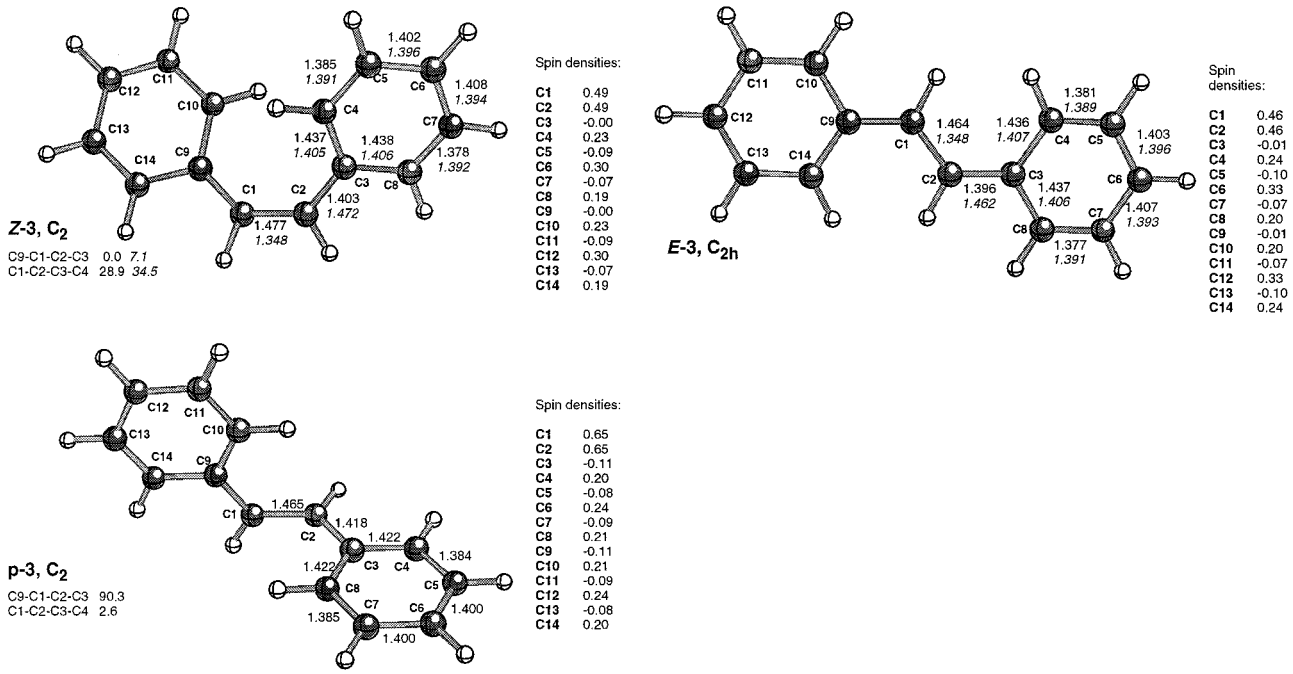

Figure 7. Geometries of stilbene (**3**) calculated at (U)B3PW91/6-31G(d) level, with values for the T_1 state in normal print, and values for the S_0 state in italics. Mulliken spin densities computed at the UBLYP/6-31G(d) level. Positive values of the atomic spin density refer to α-spin expressed in electrons.

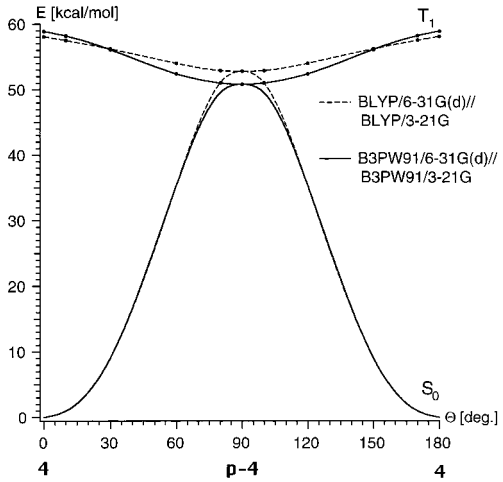

Figure 8. S_0 and T_1 potential energy surfaces for rotation around the C═C bond in 1,1-diphenylethylene (**4**) computed with UBLYP/6-31G(d)//UBLYP/3-21G (dashed lines) and UB3PW91/6-31G(d)//UB3PW91/3-21G (solid lines). The S_0 PES are schematic, interpolated from values of planar and perpendicular geometries.

also similar to the calculated value at 50.9 kcal/mol. Moreover, the stabilization of the planar structure of **4** over **1** is 21.7 kcal/mol. The T_1 energy of **4** thus resembles that of planar **2**, and no further stabilization occurs upon 1,1-diphenyl substitution.

The elongation of the C═C bond upon excitation to T_1 (0.151 Å, Figure 9) is even larger than in **2** (0.132 Å, Figure 5). The importance of quinoid-type resonance structures for the T_1 state of planar **4** is supported by findings that rotation of the phenyl groups out of the plane of the C═CH_2 fragment is smaller in T_1 than in S_0, and that the C2C3 and C2C9 bonds become partial double bonds. However, because steric congestion forces the phenyl groups in **4** out of the plane of the C═CH_2 fragment, delocalization of the radical at C2 is suppressed. Clearly, the phenyl groups are rotated to an extent so that no additional gain in stabilization of the planar structure occurs with 1,1-diphenyl substitution when compared with monophenyl substitution. The spin density at C2 is also higher in **4** than in **2**, which together with the longer C═C bond indicates that the T_1 state of planar **4** has the character of an olefin-excitation state more than the T_1 state of **2**. The shape of the second SOMO supports this interpretation because this orbital is localized to the C═C bond (Figure 3).

The energy gains upon twist of the olefin bonds in **4** and **2** are almost identical (8.0 and 8.4 kcal/mol with UB3PW91/6-31G(d); Tables 1 and 2). Because the radical at C2 is partially delocalized into both phenyl groups, relative changes in the CC bonds of these substituents as well as of the C2C3 and C2C9 bonds upon twist to p-**4** are modest. It is also notable that the spin densities at C1 and C2 in **4** hardly change upon twist. The radical character of C2 in p-**4** is therefore smaller than in p-**2** and p-**3**, and it may be questionable to classify p-**4** as a 1,2-biradical (Table 2).

Thus, 1,1-diphenyl substitution does not lead to more shallow T_1 PES because of the attenuated delocalization of the triplet biradical from the isomerizing C═C bond. It is not surprising that 1,1,2,2-tetraphenyl ethylene has a very curved T_1 PES that only admits diabatic *Z/E*-isomerizations.[40] The data from **1**−**4** clarifies that phenyl substitution on its own cannot bring an adiabatically *Z/E*-isomerizing olefin.

The spin-density distribution of planar **2** in T_1, however, reveals that certain positions of the phenyl group have more radical character than others. Placing a radical accepting group at such a position should preferentially stabilize the planar T_1 structure through further delocalization of the biradical character away from the C═C bond. Because a vinyl group is a good radical stabilizer one may expect a 1,4-divinylbenzene to have a flatter T_1 energy surface for *Z/E*-isomerization than a 1,3-divinylbenzene. For this reason we computed **5** and **6**, where 1-propenyl substituents are used in **5** because this gives a compound which T_1 PES has been determined experimentally.[41]

1,4-Bis-(1-propenyl)benzene (5). The T_1 energies of *EE*-**5**, *EZ*-**5**, and *ZZ*-**5** at UB3PW91/6-31G(d) level agree reasonably well with those from the experiment.[41] However, at this level

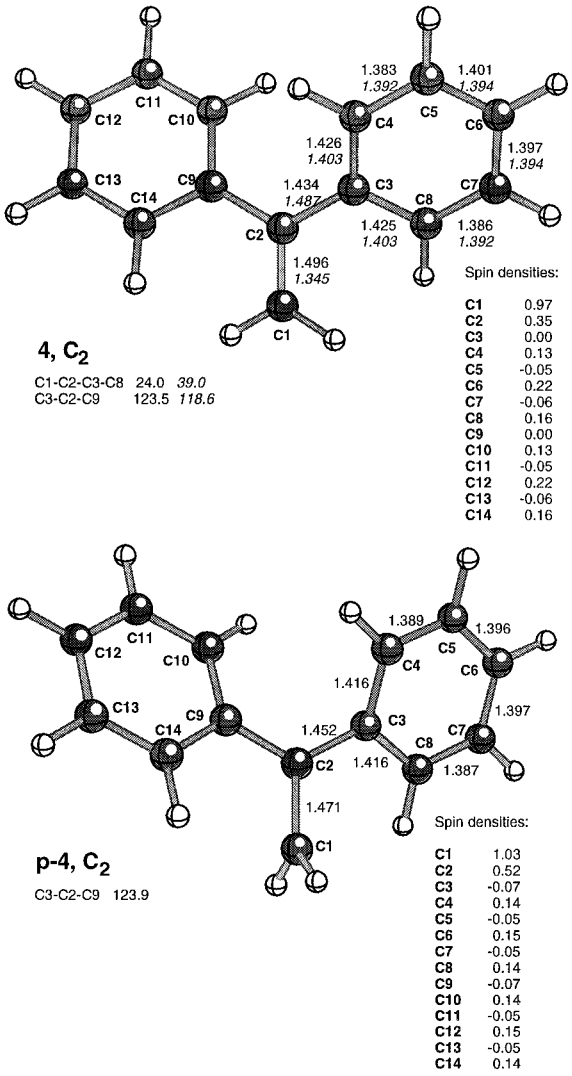

Figure 9. Geometries of 1,1-diphenylethylene (**4**) calculated at (U)B3PW91/6-31G(d) level, with values for the T_1 state in normal print, and values for the S_0 state in italics. Mulliken spin densities computed at the UBLYP/6-31G(d) level. Positive values of the atomic spin density refer to α-spin expressed in electrons.

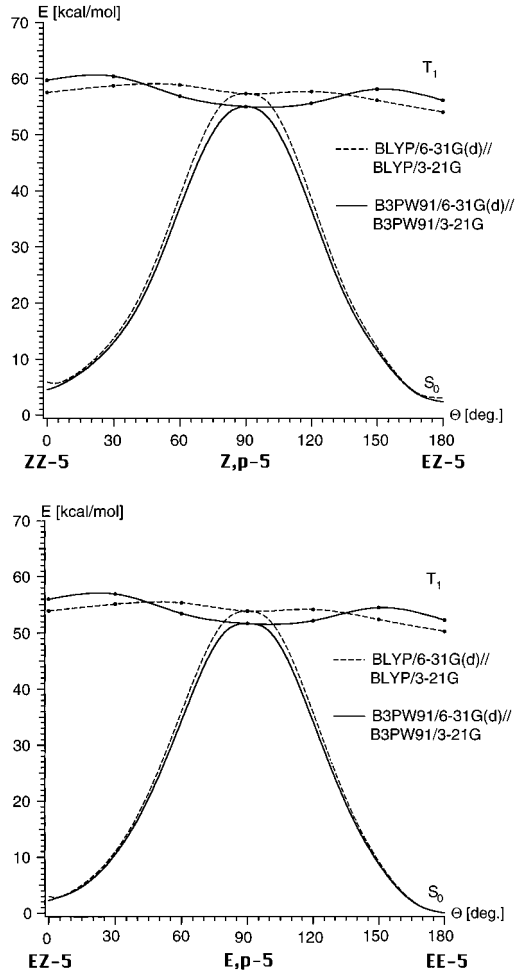

Figure 10. S_0 and T_1 potential energy surfaces for rotation around the C═C bond in 1,4-bis(1-propenyl)benzene (**5**) computed with UBLYP/6-31G(d)//UBLYP/3-21G (dashed lines) and UB3PW91/6-31G(d)//UB3PW91/3-21G (solid lines). The S_0 PES are schematic, interpolated from values of planar and perpendicular geometries.

EE-**5** is less stable than *E*p-**5** by 0.8 kcal/mol, but in the experiment *EE*-**5** was estimated to be more stable than *E*p-**5** by 1.4 kcal/mol.[41] On the other hand, because UBLYP/6-31G(d) favors *EE*-**5** by as much as 3.6 kcal/mol, the measured value for the energy difference between *EE*-**5** and *E*p-**5** is bracketed by the results from the two DFT methods.

The T_1 surfaces of **5** differ from those of **2** (Figures 10 and 4), because maxima separate the twisted and planar structures of **5**. A T_1 PES with minima at both planar and twisted structures is supported by the experiments.[41] Isomerization of **5** starting at either isomer results in a photostationary state ratio of *ZZ*/*EZ*/*EE* = 1.5:49:49.5, with decay mainly from *E*p-**5**. However, addition of azulene as quencher results in a drastic increase of *EE*-**5** in the photostationary state (the ratio *EZ*/*EE* is 9.8:90.2 with no formation of *ZZ*).[41] This indicates an equilibrium between *E*p-**5** and *EE*-**5**, and with the two species being rather isoenergetic as found in our calculations. In S_0, the energy difference between *EE*-**5** and *ZZ*-**5** is 4.7−6.0 kcal/mol and it is 5.2−7.4 kcal/mol in T_1. Thus, the steric strain in *ZZ*-**5** is similar in the two states, so that considerable energy is released when going from *Z*- to *E*-arrangements, favoring *E*p-**5** and *EE*-**5** as the dominant species in T_1.

The energy of ^{3}p* structures of styrenes seem unaffected by a radical stabilizing group in para-position, because the UB3PW91/6-31G(d) energies of p-**2** and *E*p-**5** are similar within 1.4 kcal/mol (Table 2). However, the energy difference between planar **2** and *EE*-**5** is 9.0 kcal/mol at the same level of computation. Preferential stabilization of planar styrenes, and a more shallow T_1 PES, is therefore achieved by attachment of an olefinic or other radical-stabilizing group in para-position. Positioning of radical stabilizers, which are not sterically congestive, also in ortho-positions may lead to T_1 PESs with maxima at ^{3}p*.

The involvement of a doubly twisted pp-**5** could be excluded in the experiments.[41] At the UB3PW91/6-31G(d) level, the analogous structure of 1,4-divinylbenzene is 33.2 kcal/mol above the planar T_1 structure, supporting the conclusion that pp-**5** has no importance for the T_1 photochemistry of **5**.

In T_1, each of the two C═C bonds in *EE*-**5** are elongated by half of the value in **2** (0.053 Å in *EE*-**5** and 0.132 Å in **2**; Figures 11 and 5). Thus, the elongation of each C═C bond is merely 25% of that of a full olefin excitation. However, the T_1 excitation is symmetrically delocalized over both C═C bonds so that the total change is similar to that in **2**. The C═C bonds for *Z*-arrangements are slightly longer than for *E*-arrangements, but relative bond length changes upon excitation of *EZ*-**5** and *ZZ*-**5** are similar to those in the *EE*-isomer.

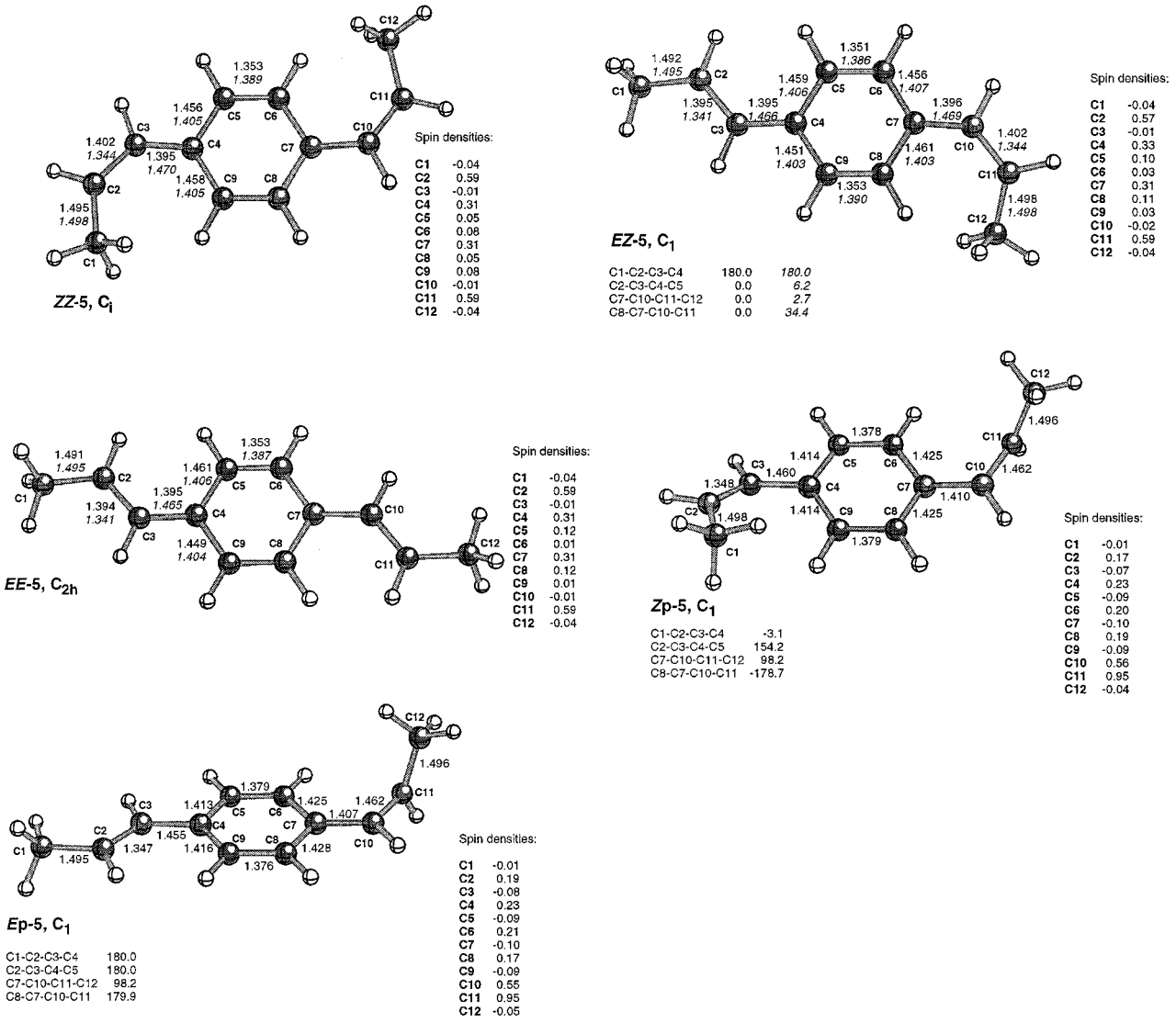

Figure 11. Geometries of 1,4-bis(1-propenyl)benzene (**5**) calculated at the (U)B3PW91/6-31G(d) level, with values for the T_1 state in normal print, and values for the S_0 state in italics. Mulliken spin densities computed at the UBLYP/6-31G(d) level. Positive values of the atomic spin density refer to α-spin expressed in electrons.

For *EE*-**5**, the variation in the CC bond distances within the benzene ring in S_0 is 0.033 and 0.114 Å in T_1, similar as in **2** (0.086 Å). The shortening of the C3C4 and C7C10 bonds upon excitation to T_1 is less dramatic than in **2** (0.063 Å in *EE*-**5** vs 0.094 Å in **2**), but these geometry changes still reveal that quinoid-type resonance structures are important in planar T_1 isomers of **5**. In all planar T_1 structures of **5**, the spin density is mainly located at C2 and C11 with spreads to C4 and C7 (Figure 11). This shows that the two unpaired electrons prefer to be as distant as possible, and the excitation should be regarded as a delocalized olefin excitation. The shape of the second SOMO supports this view because the slight localization to the C═C bond that occurred in **2**−**4** is not seen in **5** (Figure 3). Instead, this orbital is evenly spread over the molecule, in line with expectations for an olefin that isomerizes with a dual mechanism.

Upon twist from *EE*-**5** to *E*p-**5** the variation in CC bond lengths within the phenyl group is reduced to 0.052 Å, and the nonisomerizing propenyl group adopts its S_0 geometry. Thus, the para-positioned 1-propenyl group serves no role as a stabilizer in ^{3}p* structures, as concluded above. Moreover, the recovery of aromaticity of the benzene ring is obvious, even though it is less distinct than in **2**. Partial 1,2-biradicals are formed in *E*p-**5** and *Z*p-**5** which resemble that of p-**2** because the spin densities at C10 and C11 in *E*p-**5** and *Z*p-**5** resemble those of C2 and C1 in p-**2**, respectively.

1,3-Divinylbenzene (6). A comparison of **5** (and 1,4-divinylbenzene) with 1,3-divinylbenzene (**6**) shows the importance of the position of the radical-stabilizing group for the shape of the T_1 PES. In **6**, radical delocalization from one vinyl group to the other is not possible so that stabilization of the planar T_1 structure should be smaller than in styrenes with olefinic substituents in 2- and/or 4-positions.

Because no experimental data exist for **6,** our analysis relies solely on computations. In line with expectations, the T_1 energy of planar **6** with the DFT methods is higher than that of *EE*-**5** by 8−10 kcal/mol, and it therefore resembles that of **2**. The planar T_1 structure also corresponds to a transition state in analogy with **2**. The minimum on the T_1 PES is located at the p-**6** structure, so that it has a shape suitable for pure diabatic *Z/E*-isomerizations (Figure 12).

The optimal T_1 geometry of planar **6** shows that the excitation becomes localized to one of the vinyl groups (Figure 13), and this C═C bond is elongated to the same extent as in planar **2** (0.132 Å in **2** and 0.131 Å in **6**). Moreover, the spin densities in the benzene ring, and in the vinyl group to which the

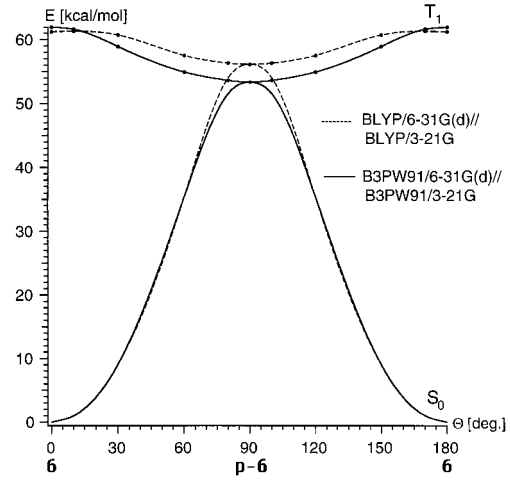

Figure 12. S_0 and T_1 potential energy surfaces for rotation around the C═C bond in 1,3-divinylbenzene (**6**) computed with UBLYP/6-31G(d)//UBLYP/3-21G (dashed lines) and UB3PW91/6-31G(d)//UB3PW91/3-21G (solid lines). The S_0 PES are schematic, interpolated from values of planar and perpendicular geometries.

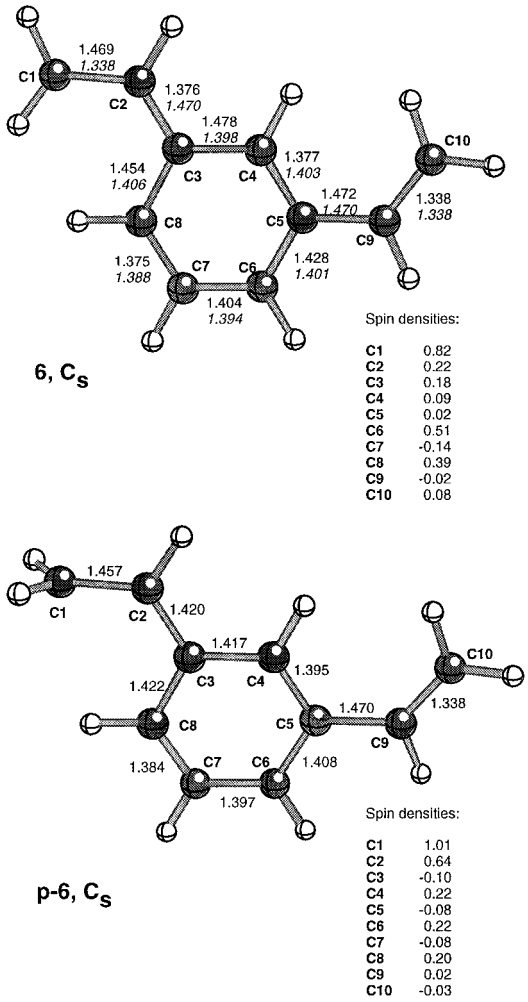

Figure 13. Geometries of 1,3-divinylbenzene (**6**) calculated at (U)B3PW91/6-31G(d) level, with values for the T_1 state in normal print, and values for the S_0 state in italics. Mulliken spin densities computed at the UBLYP/6-31G(d) level. Positive values of the atomic spin density refer to α-spin expressed in electrons.

excitation has been localized, are similar in **6** and **2**. On the other hand, the geometry and spin-density distribution of the nonisomerizing C═C bond remains as in S_0. The shape of the

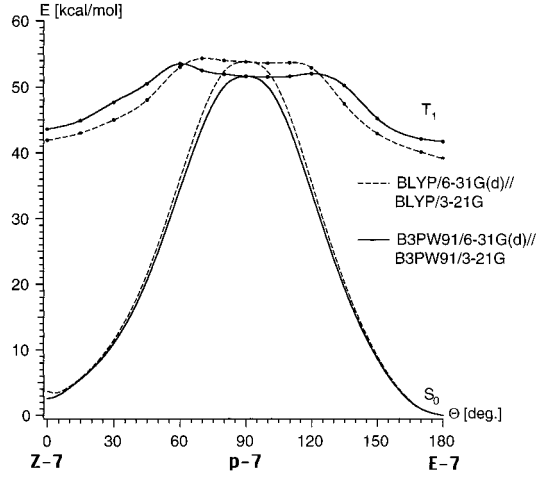

Figure 14. S_0 and T_1 potential energy surfaces for rotation around the C═C bond in 2-(1-propenyl)anthracene (**7**) computed with UBLYP/6-31G(d)//UBLYP/3-21G (dashed lines) and UB3PW91/6-31G(d)//UB3PW91/3-21G (solid lines). The S_0 PES are schematic, interpolated from values of planar and perpendicular geometries.

second SOMO as an indicator of excitation localization is not appropriate for **6**. However, the first SOMO (∼HOMO in S_0) has very little bonding character in one of the vinyl groups (Figure 3) and cannot compensate for the antibonding character of the second SOMO, leading to a C═C bond elongation upon excitation to T_1.

However, p-**6** is isoenergetic with p-**2** and *E*p-**5**. Because ^{3}p* structures are mainly 1,2-biradicals, additional substitution of olefin substituents has little influence on relative stabilities of such structures. The isomerizing C═C bond is shortened upon twist, whereas the nonisomerizing vinyl group stays intact. As in previous cases and especially in **2**, the variation in CC bond lengths within the benzene ring decreases from 0.103 to 0.038 Å.

Through the comparison of **5** and **6** it becomes clear that excitation delocalization reduces the diabatic character of *Z/E*-isomerizations. In a photochemical sense, **6** is merely a styrene derivative, whereas **5** is a molecule with a separate photochemistry. In general, radical-stabilizing groups at proper positions of an aryl-substituted olefin could alter the shape of the T_1 PES to the extent that the *Z/E*-isomerization mechanism is changed. However, because a vinyl group is a good radical stabilizer, maximum stabilization of planar phenyl-substituted olefins could have been reached with **5** and other derivatives of 1,4-divinylbenzene.

2-(1-Propenyl)anthracene (7). A different approach to achieve less excitation localization in the rotating C═C bond, and a T_1 PES that favors adiabatic isomerizations, is the use of an olefin substituent whose T_1 energy is sufficiently low so that the excitation becomes localized to this part.[2] This has been termed ring excitation[2] and is exemplified by **7**. A comparison of energies, geometries, and spin densities of planar and twisted forms of **1**, **2**, and **7** gives information on characteristics of the electronic structure of diabatically vs adiabatically isomerizing olefins.

The T_1 energy of *E*-**7** at UB3PW91/6-31G(d) level is very close to those measured for 2-(ethenyl)anthracene and 2-(3,3-dimethyl-1-butenyl)anthracene, even though the energy for the ^{3}p* structure is lower by 1−2 kcal/mol (Table 2).[2,9] The shape of the T_1 surface at UB3PW91 level is in excellent agreement with the measured surfaces.

The calculated T_1 PES thus allow for an adiabatic isomerization mechanism (Figure 14). There is a shallow minimum at

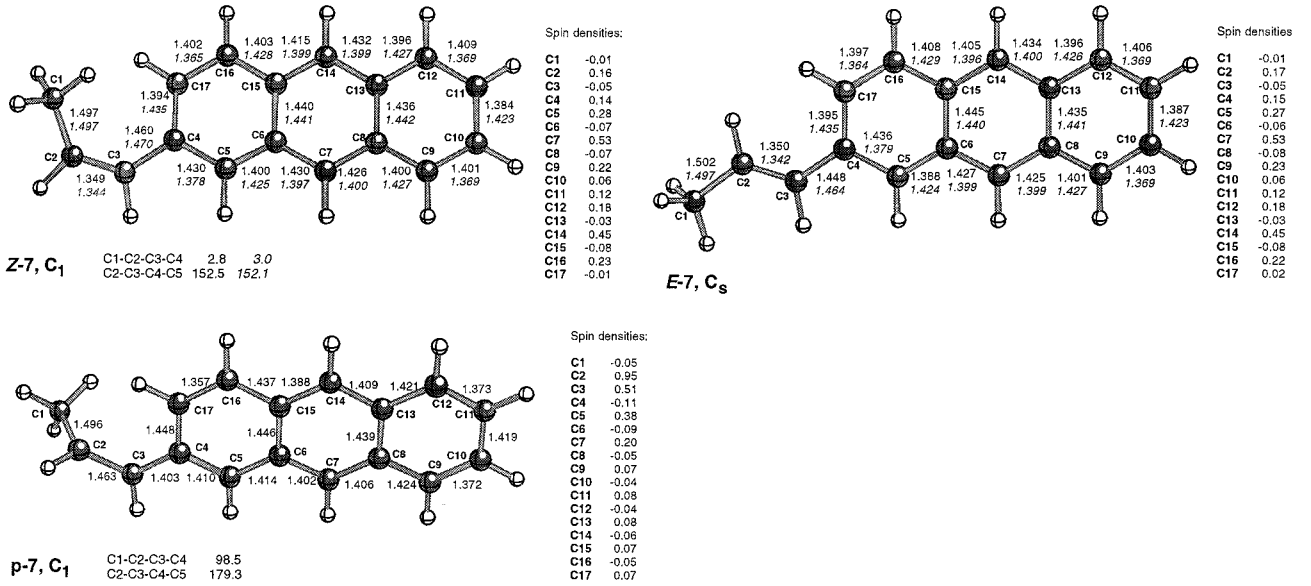

Figure 15. Geometries of 2-(1-propenyl)anthracene (**7**) calculated at the (U)B3PW91/6-31G(d) level, with values for the T_1 state in normal print, and values for the S_0 state in italics. Mulliken spin densities computed at the UBLYP/6-31G(d) level. Positive values of the atomic spin density refer to α-spin expressed in electrons.

p-**7** but the relaxation to the planar conformers is presumably faster than the rate for intersystem crossing to the ground state. The energy difference between the *E*- and *Z*-isomer in S_0 is 3.2 kcal/mol with B3PW91/6-31G(d). In the T_1 state this difference is slightly smaller (1.9 kcal/mol), which shows that steric congestion in the *Z*-isomer is in part transferred from S_0 to T_1.

When compared with **1**, the stabilizations of planar and perpendicular T_1 structures of **7** are 39−46 kcal/mol and 10−12 kcal/mol (Tables 1 and 2). Because the triplet energies of p-**2**, p-**4**, *E*p-**5**, p-**6**, and p-**7** differ by only 2−3 kcal/mol, the relative stabilization of ^{3}p* is not significantly influenced by size and triplet energy of the olefin substituent. The anthryl group predominantly lowers the T_1 energy of the planar structure. Instead, ^{3}p* structures are stabilized when aryl groups are attached to both sides of the 1,2-biradical, as shown by the energies for the successive series p-**1**, p-**2**, and p-**3**. This is also known from styrylanthracenes, which have shallower T_1 PES than, for example, 2-(ethenyl)anthracene.[2,7]

Upon excitation to T_1 the olefinic bond of *E*-**7** is elongated by 0.008 Å (Figure 15), merely ∼4% of the elongation found in **1**. Clearly, the excitation is localized in the anthryl system. Moreover, the C3C4 bond, which in T_1 becomes a partial double bond in **2**−**6**, has a similar length in both S_0 and T_1. Negligible bond-length changes in the 1-propenyl part of the molecule are also seen for *Z*-**7**, so that the destabilization of this isomer due to steric repulsion is similar in T_1 and S_0.

The differences between the longest and shortest CC bonds of the aromatic system are noteworthy. For the whole anthryl group in *E*-**7**, the difference is 0.077 Å in S_0 and 0.058 Å in T_1. If the C6C15 and C8C13 bonds are disregarded, the values are 0.071 and 0.049 Å. If each ring is regarded separately, the differences in CC bond length in the S_0 state are 0.076, 0.045, and 0.072 Å, to be compared with 0.057, 0.040, and 0.048 Å in T_1. Thus, the difference between longest and shortest CC bond in *E*-**7** decreases upon excitation from S_0 to T_1, and it seems as if the anthryl group is more aromatic in T_1 than in S_0.

The spin density at the UBLYP/6-31G(d) level shows that the two unpaired electrons in the planar T_1 structures of **7** in T_1 are somewhat localized to C7 and C14, in line with conclusions of Tokumaru and co-workers.[14] Thus, the two outer benzene rings keep their aromaticity in the planar T_1 structures. The ability of an anthryl group to accommodate a triplet biradical, and simultaneously retain substantial aromaticity, is a key factor to the low T_1 energies of anthryl-substituted olefins in comparison with, for example, phenanthryl-substituted olefins.

Upon twist from *E*-**7** to p-**7** in T_1, the olefinic bond lengthens by 0.113 Å and the C3C4 bond shortens by 0.045 Å. Moreover, the CC bond distances within the anthryl group approach their ground-state values, even though some bonds in their reduction (elongation) processes become shorter (longer) than in S_0. The difference between longest and shortest CC bond in the anthryl group of p-**7** is 0.091 Å.

In p-**7**, C2 receives a considerable amount of spin density, so that one of the radicals is located at this atom. The C3 atom also receives spin density, but to a smaller extent than in **2**. The second unpaired electron is instead partly delocalized into the anthryl group, and it is not fully satisfactory to describe p-**7** as a 1,2-biradical. It becomes clear that upon rotation from *E*- and *Z*-**7** to p-**7** in T_1, the aromaticity of the outer benzene rings in the anthryl group is disrupted. This causes the energy to increase at p-**7**, and the T_1 PES to adopt a shape that admits an adiabatic *Z/E*-isomerization.

Finally, the second SOMO of **7** is localized in the anthryl group (Figure 3). The lobe of this orbital at C3 is small, and its antibonding character in the olefinic bond is negligible so that the elongation of this bond upon excitation to T_1 is minute. Because the first SOMO has a large lobe in the C2C3 bond, and because this orbital is singly occupied in T_1, the π-bonding is still considerable in this state. 2-(1-Propenyl)anthracene therefore is an example of a substituted olefin where the T_1 state is a ring-excited state and for which the *Z/E*-isomerization proceeds adiabatically.

Generalization and Summary

The T_1 energies of the olefins **1**−**7** calculated using the density functional methods BLYP and B3PW91 are in good agreement with experimental data (≤5.5 kcal/mol), and the computed T_1 PES of the seven molecules exhibit the shapes determined experimentally. The B3PW91 method reproduces the shape of the T_1 PES slightly better than BLYP. The worst agreement, both qualitatively and quantitatively, is obtained with

ROHF. Because of the agreement between DFT computations and experiments, calculated properties of **1**−**7** can be used to analyze which electronic factors determine the shape of T_1 PES of olefin *Z/E*-isomerizations.

Starting with geometries, there is a good correlation (r = 0.96) between the elongation of the C═C bond upon excitation from S_0 to T_1 and the shape of the T_1 PES, measured as the energy difference between $^3E^*$ and $^3p^*$. In our two extremes of diabatically and adiabatically isomerizing olefins, **1** and **7**, the elongations upon excitation are 0.208 and 0.008 Å, respectively. These represent the pure olefin- and ring-excited T_1 states, as previously noted by Tokumaru et al.[14] However, the elongation of the isomerizing C═C bond in $^3E^*$ and $^3Z^*$ structures decreases gradually with increasing adiabaticity of the isomerization, and only the T_1 excitation in **1** is a pure olefin excitation. At the $^3p^*$ structures, the olefins **1**−**7** adopt C═C bond lengths in the narrow range of 1.449−1.471 Å, which simply shows that the two radical parts of these structures do not interact significantly.

We also considered geometry changes of the aryl groups upon excitation to T_1, as well as along the isomerization path. The differences between longest and shortest CC bonds in the phenyl groups of **2**−**6** increase dramatically when going from S_0 to T_1. Because molecules (groups) that are aromatic in S_0 become antiaromatic in T_1, and vice versa,[20,21] the antiaromatic character of the phenyl group in T_1 is alleviated by alternating CC bond lengths. However, the aromaticity of the phenyl groups is partially regained when going from $^3E^*$/ $^3Z^*$ to $^3p^*$ because the CC bond lengths equalize. The changes in aromaticity along T_1 PES are also supported by the calculated spin densities. In the planar triplet structures the delocalization of spin density to the substituents is significant, whereas the $^3p^*$ structures of **2**−**6** should be partially considered as 1,2-biradicals. The latter finding is in line with conclusions of Caldwell and Zhou.[35]

The situation is opposite for **7**. Anthracene has a low triplet energy because part of its aromaticity is conserved when the biradical character is localized to the middle ring.[14] The spin-density distribution confirms that the unpaired electrons are partially localized to the middle ring in both $^3E^*$ and $^3Z^*$ structures of **7**. The geometry changes that occur upon excitation of **7** indicate that the anthryl group is still aromatic in planar T_1 structures. However, upon twist to p-**7** the aromaticity of one of the outer rings must be disrupted, which leads to an energy increase and an adiabatic T_1 PES.

Because the two unpaired electrons in T_1 anthracene reside in the middle benzene ring, the positioning of the olefin onto the anthryl system will have an impact on how the olefin isomerizes. With the olefin in 9-position, the aromaticity of the two outer benzene rings of the anthryl group is kept intact when going from a planar T_1 structure to $^3p^*$. However, for those vinylanthracenes with the C═C bond in 1- or 2-position, the aromaticity is reduced when going to $^3p^*$. This should lead to a flatter T_1 PES for 9-vinylanthracenes than for 1- and 2-vinylanthracenes, in line with observations of Tokumaru, Arai, and co-workers.[42]

Thus, our study indicates that the change in substituent aromaticity along the isomerization pathway is connected to the shape of the T_1 PES. Aryl substituents on olefins that isomerize diabatically regain parts of their aromaticity when going from $^3E^*$/ $^3Z^*$ to $^3p^*$, so that the energy is lowered when the olefin twists. The opposite is true for aryl-substituted olefins that isomerize adiabatically. Thus, that point on the T_1 surface with the highest substituent aromaticity seems to correspond to the minimum. This finding indicates that T_1 *Z/E*-isomerizations of olefins with substituents that are antiaromatic in S_0 and aromatic in T_1 (e.g., cyclobutadienyl)[20,21] proceed adiabatically. We are currently investigating the relationship between substituent aromaticity and shape of the T_1 PES. Our computations show that vinylcyclobutadiene isomerizes over a barrier of 19.4 kcal/mol at the UB3PW91/6-31G(d,p) level, in support of the importance of substituent aromaticity for the shape of the T_1 PES, and presumably also the isomerization mechanism.[43]

The computed spin-density distributions revealed that the two unpaired electrons of a T_1 excited olefin reside at certain positions in the molecule. For this reason, it should be possible to stabilize a particular structure of a triplet olefin by attaching radical-stabilizing groups at these positions. The para-positions of the phenyl groups of **2**, **3**, and **4** obtain high spin densities in the planar T_1 structures. As verified through comparison of **2**, **5**, and **6**, the effect of a radical stabilizer in lowering the energy of $^3E^*$ structures is greater when attached in a para- than in a meta-position.

Because the two unpaired electrons in a triplet olefin do not interact, similar modes of stabilization should apply to olefins in T_1 and to carbenes in their ^3B and ^1B states, and knowledge gained from such carbenes can be transferred to T_1 olefins. In an electron spin resonance study of triplet diphenylcarbenes, Tomioka and co-workers recently found that para-nitro and para-cyano groups exhibit significant stabilizing effects.[44] This parallells the finding of radical stabilization in **5**. One could therefore expect that the $^3E^*$ and $^3p^*$ structures of 4,4′-dinitrostilbene, for example, are more isoenergetic than in parent stilbene. Indeed, UB3PW91/6-31G(d)//UB3PW91/3-21G calculations show that $^3p^*$ is lower than $^3E^*$ by just 1.7 kcal/mol, to be compared with 4.1 kcal/mol for parent stilbene (**3**). At the corresponding UBLYP level the stability order is even reversed, because $^3p^*$ is higher in energy than $^3E^*$ by 2.3 kcal/mol. The T_1 state *Z/E*-isomerization of 4,4′-dinitrostilbene was investigated previously.[45,46] An equilibrium between $^3E^*$ and $^3p^*$ structures was revealed, and the triplet lifetime was longer than for parent stilbene. This supports our computations that T_1 energies of $^3E^*$ and $^3p^*$ of 4,4′-dinitrostilbene are more isoenergetic than in stilbene.

Finally, because T_1 states of olefins are mainly described by the electron configuration in which an electron is lifted from HOMO to LUMO, the shapes of the two SOMOs can be used as rough indicators for excitation localization. For molecules that undergo diabatic isomerization, the excitation is slightly more localized in the isomerizing C═C bond (i.e., olefin excitation), whereas molecules undergoing adiabatic isomerization have the excitation localized to the aryl group (i.e., ring excitation).

Acknowledgment. All calculations were performed on the CRAY C90 computer of Nationellt Superdatorcentrum (NSC) in Linköping, Sweden. The authors acknowledge NSC for a generous allotment of computer time. Financial support from the Swedish Council for Engineering Sciences (TFR), the Swedish Natural Science Research Council (NFR), and the Wenner-Gren Foundations is also gratefully acknowledged.

Supporting Information Available: Table of absolute energies (2 pages) at UBLYP/6-31G(d)//UBLYP/3-21G, UBLYP/6-31G(d), UB3PW91/6-31G(d)//UB3PW91/3-21G, and UB3PW91/6-31G(d) levels for the optimal S_0 and T_1 structures shown in figures. This material is available free of charge via the Internet at http://pubs.acs.org.

References and Notes

(1) For overviews of *Z/E*-photoisomerization of olefins see: (a) Saltiel, J.; Sun, Y.-P. In *Photochromism: Molecules and Systems*; Dürr, H., Bouas-Laurent, H., Eds.; Elsevier: Amsterdam, 1990; p 64. (b) Görner, H.; Kuhr, H. J. *Adv. Photochem*. **1995**, *19*, 1.

(2) For reviews on adiabatic triplet state *Z/E*-photoisomerizations see: (a) Arai, T.; Tokumaru, K. *Chem. Rev.* **1993**, *93*, 23. (b) Arai, T.; Tokumaru, K. *Adv. Photochem.* **1995**, *20*, 1. (c) Arai, T. In *Organic Molecular Photochemistry*; Ramamurthy, V., Schanze, K. S., Eds.; Marcel Dekker: New York, **1999**; p 131.

(3) Rando, R. A. *Angew. Chem., Int. Ed. Engl.* **1990**, *29*, 461

(4) Kanna, Y.; Arai, T.; Tokumaru, K. *Bull. Chem. Soc. Jpn.* **1993**, *66*, 1482.

(5) Sundahl, M.; Wennerström, O. *J. Photochem. Photobiol. A* **1996**, *98*, 117.

(6) Brink, M.; Jonson, H.; Sundahl, M. *J. Photochem. Photobiol. A* **1998**, *112*, 149.

(7) Tokumaru, K.; Arai, T. *J. Photochem. Photobiol. A* **1992**, *65*, 1.

(8) (a) Bartocci, G.; Mazzucato, U.; Spalletti, A.; Orlandi, G.; Poggi, G. *J. Chem. Soc., Faraday Trans.* **1992,** *88*, 3139. (b) Orlandi, G.; Negri, F.; Mazzucato, U.; Bartocci, G. *J. Photochem. Photobiol. A* **1990**, *55*, 37.

(9) (a) Arai, T.; Karatsu, T.; Sakuragi, H.; Tokumaru, K. *Tetrahedron Lett.* **1983**, *24*, 2873. (b) Hamaguchi, H.; Tasumi, M.; Karatsu, T.; Arai, T.; Tokumaru, K. *J. Am. Chem. Soc.* **1986**, *108*, 1698. (c) Misawa, H.; Karatsu, T.; Arai, T.; Sakuragi, H.; Tokumaru, K. *Chem. Phys. Lett.* **1988**, *146*, 405.

(10) Said, M.; Malrieu, J. P. *Chem. Phys. Lett.* **1983**, *102*, 312.

(11) Orlandi, G.; Poggi, G. *J. Photochem.* **1986**, *35*, 289.

(12) Langkilde, F. W.; Wilbrandt, R.; Brouwer, A. M.; Negri, F.; Zerbretto, F.; Orlandi, G. *J. Phys. Chem*. **1994**, *98*, 2254.

(13) Bartocci, G.; Masetti, F.; Mazzucato, U.; Spalletti, A.; Orlandi, G.; Poggi, G. *J. Chem. Soc., Faraday Trans. 2* **1988**, *84*, 385.

(14) (a) Kikuchi, O.; Segawa, K.; Takahashi, O.; Arai, T.; Tokumaru, K. *Bull. Chem. Soc. Jpn*. **1992**, *65*, 1463. (b) Segawa, K.; Takahashi, O.; Kikuchi, O.; Arai, T.; Tokumaru, K. *Bull. Chem. Soc. Jpn*. **1993**, *66*, 2754.

(15) Brink, M.; Jonson, H.; Ottosson, C.-H. *J. Phys. Chem. A* **1998**, *102*, 6513.

(16) Negri, F.; Orlandi, G. *J. Photochem. Photobiol. A* **1997**, *105*, 209.

(17) (a) Cramer, C. J.; Dulles, F. J.; Falvey, D. *J. Am. Chem. Soc.* **1994**, *116*, 9787. (b) Cramer, C. J.; Dulles, F. J.; Storer, J. W.; Worthington, S. E. *Chem. Phys. Lett.* **1994**, *218*, 387. (c) Cramer, C. J.; Dulles, F. J.; Giesen, D. J.; Almlöf, J. *Chem. Phys. Lett.* **1995**, *245*, 165. (d) Cramer, C. J.; Worthington, S. E. *J. Phys. Chem.* **1995**, *99*, 1462. e) Cramer, C. J.; Smith, B. A. *J. Phys. Chem.* **1996**, *100*, 9664.

(18) Bérces, A.; Zgierski, M. Z. *Chem. Phys. Lett.* **1996**, *257*, 61.

(19) (a) Bottinger, H. F.; Schreiner, P. R.; Schleyer, P. v. R.; Schaefer, H. F. III *J. Phys. Chem.* **1996**, *100*, 16147 (b) Xie, Y.; Schreiner, P. R.; Schleyer, P. v. R.; Schaefer, H. F. *J. Am. Chem. Soc.* **1997**, *119*, 1370.

(20) Gogonea, V.; Schleyer, P. v. R.; Schreiner, P. R. *Angew. Chem., Int. Ed. Engl.* **1998**, *37*, 1945.

(21) Baird, N. C. *J. Am. Chem. Soc.* **1972**, *94*, 4941.

(22) Becke, A. D. *Phys. Rev. A* **1988**, *38*, 3098

(23) Becke, A. D. *J. Chem. Phys.* **1993**, *98*, 5648.

(24) Lee, C.; Yang, W.; Parr, R. G. *Phys. Rev. B* **1988**, *37*, 785.

(25) Perdew, J. P.; Wang, Y. *Phys. Rev. B* **1992**, *45*, 13244.

(26) Binkley, J. S.; Pople, J. A.; Hehre, W. J. *J. Am. Chem. Soc*. **1980**, *102*, 939.

(27) Hariharan, P. C.; Pople, J. A. *Theor. Chim. Acta* **1973**, *28*, 213.

(28) (a) Frisch, M. J.; Trucks, G. W.; Schlegel, H. B.; Gill, P. M. W.; Johnson, B. G.; Robb, M. A.; Cheeseman, J. R.; Keith, T.; Petersson, G. A.; Montgomery, J. A.; Raghavachari, K.; Al-Laham, M. A.; Zakrzewski, V. G.; Ortiz, J. V.; Foresman, J. B.; Peng, C. Y.; Ayala, P. Y.; Chen, W.; Wong, M. W.; Andres, J. L.; Replogle, E. S.; Gomperts, R.; Martin, R. L.; Fox, D. J.; Binkley, J. S.; Defrees, D. J.; Baker, J.; Stewart, J. P.; Head-Gordon, M.; Gonzalez, C.; Pople, J. A. *Gaussian 94*, Revision C.3; Gaussian, Inc.: Pittsburgh, PA, 1995. (b) Frisch, M. J.; Trucks, G. W.; Schlegel, H. B.; Scuseria, G. E.; Robb, M. A.; Cheeseman, J. R.; Zakrzewski, V. G.; Montgomery, J. A. Jr.; Stratmann, R. E.; Burant, J. C.; Dapprich, S.; Millam, J. M.; Daniels, A. D.; Kudin, K. N.; Strain, M. C.; Farkas, O.; Tomasi, J.; Barone, V.; Cossi, R.; Cammi, R.; Mennucci, B.; Pomelli, C.; Adamo, C.; Clifford, S.; Ochterski, J.; Petersson, G. A.; Ayala, P. Y.; Cui, Q.; Morokuma, K.; Malick, D. K.; Rabuck, A. D.; Raghavachari, K.; Foresman, J. B.; Cioslowski, J.; Ortiz, J. V.; Stefanov, B. B.; Liu, G.; Liashenko, A.; Piskorz, P.; Komaromi, I.; Gomberts, R.; Martin, R. L.; Fox, D. J.; Keith, T.; Al-Laham, M. A.; Peng, C. Y.; Nanayakkara, A.; Gonzalez, C.; Challacombe, M.; Gill, P. M. W.; Johnson, B.; Chen, W.; Wong, M. W.; Andres, J. L.; Head-Gordon, M.; Replogle, E. S.; Pople, J. A. *Gaussian 98*, Revision A.3; Gaussian, Inc.: Pittsburgh, PA, 1998.

(29) Evans, D. *J. Chem. Soc.* **1960**, 1735.

(30) Gemein, B.; Peyerimhoff, S. D. *J. Phys. Chem*. **1996**, *100*, 19257.

(31) Ni, T.; Caldwell, R. A.; Melton L. A. *J. Am. Chem. Soc.* **1989**, *111*, 457.

(32) Evans, D. F. *J. Chem. Soc.* **1957**, 1351.

(33) (a) Hemley, R. J.; Dinur, U.; Vaida, V.; Karplus, M. *J. Am. Chem. Soc.* **1985**, *107*, 836. (b) Orlandi, G.; Palmieri, P.; Poggi, G. *J. Chem. Soc., Faraday Trans. 2* **1981**, *77*, 71. (c) Bearpark, M. J.; Olivucci, M.; Wilsey, S.; Bernardi, F.; Robb, M. A. *J. Am. Chem. Soc.* **1995**, *117*, 6944.

(34) Kellogg, R. E.; Simpson, W. T. *J. Am. Chem. Soc.* **1965**, *87*, 4230.

(35) Caldwell, R. A.; Zhou, L. *J. Am. Chem. Soc.* **1994**, *116*, 2271.

(36) (a) Saltiel, J.; Rousseau, A. D.; Thomas, B. *J. Am. Chem. Soc.* **1983**, *105*, 7631. (b) Saltiel, J.; Ganapathy, S.; Werking, C. *J. Phys. Chem.* **1987**, *91*, 2755.

(37) (a) Görner, H.; Schulte-Frohlinde, D. *J. Phys. Chem.* **1979**, *83*, 3107. (b) Görner, H.; Schulte-Frohlinde, D. *J. Phys. Chem*. **1981**, *85*, 1835.

(38) (a) Langkilde, F. W.; Wilbrandt, R.; Negri, F.; Orlandi, G. *Chem. Phys. Lett.* **1990**, *165*, 66. (b) Langkilde, F. W.; Wilbrandt, R.; Brouwer, A. M.; Negri, F.; Zerbetto, F.; Orlandi, G. *J. Phys. Chem.* **1994**, *98*, 2254.

(39) Langkilde, F.; Wilbrandt, R.; Brouwer, A. M.; Jacobs, H. J. C.; Negri, F.; Orlandi, G. *J. Phys. Chem.* **1992**, *96*, 64.

(40) Caldwell, R. A.; Unett, D. J.; Vipond, J. J. *Photochem. Photobiol.* **1997**, *65*, 530.

(41) Jonson, H.; Sundahl, M. *J. Photochem. Photobiol. A* **1996**, *93*, 145.

(42) (a) Karatsu, T.; Kitamura, A.; Zeng, H.; Arai, T.; Sakuragi, H.; Tokumaru, K. *Chem. Lett.* **1992**, 2193. (b) Karatsu, T.; Misawa, H.; Nojiri, M.; Nakahigashi, N.; Watanabe, S.; Kitamura, A.; Arai, T.; Sakuragi, H.; Tokumaru, K. *J. Phys. Chem.* **1994**, *98*, 508.

(43) Brink, M.; Möllerstedt, H.; Ottosson, C.-H. Submitted for publication.

(44) (a) Hu, Y.; Hirai, K.; Tomioka, H. *J. Phys. Chem. A* **1999**, *103*, 9280. (b) Hu, Y.; Hirai, K.; Tomioka, H. *Chem. Lett.* **2000**, 94.

(45) (a) Görner, H. *Ber. Bunsen-Ges. Phys. Chem.* **1984**, *88*, 1199. (b) Görner, H.; Schulte-Frohlinde, D. *Ber. Bunsen-Ges. Phys. Chem.* **1984**, *88*, 1208.

(46) Smit, K. J. *J. Phys. Chem.* **1992**, *96*, 6555.